Corrosion Behavior and Tensile Properties of AISI 316LN Stainless Steel Exposed to Flowing Sodium at 823 K

S. Rajendran Pillai, N. Sivai Barasi, H.S. Khatak, A.L.E. Terrance, R.D. Kale, M. Rajan, and K.K. Rajan

(Submitted 17 February 1999; in revised form 14 October 1999)

Austenitic stainless steel of the grade AISI 316 LN was exposed to flowing sodium in a loop at 823 K for 6,000 h to examine the corrosion and mass-transfer behavior. The specimens were incorporated in specially designed sample holders in the loop. These were retrieved and examined by various metallurgical techniques. Specimens were also subjected to thermal aging in the same sample holder to aid in separating the consequences of exposure to sodium from those cause by mere thermal effects. Microstructural investigations have revealed that thermal aging caused the precipitation of carbides at the grain boundaries. Exposure to sodium caused the leaching of elements such as chromium and nickel from the specimen. Loss of nickel from the austenite phase promoted the generation of ferrite phase. Microhardness investigation revealed the hardening of the sodium-exposed surface. Analysis using an electron Probe Microanalyzer revealed that the surface of the steel was both carburized and nitrided. Tensile tests indicated that there is no appreciable difference in the yield strength (YS) and ultimate tensile strength (UTS) of the thermally aged and sodium-exposed specimens when compared with the material in the as-received condition. However, the thermally aged and sodium-exposed specimens showed a decrease in the uniform elongation and total elongation at rupture, perhaps due to carburization and nitridation.

Keywords compatibility, molten sodium, stainless steel, steel, tensile strength

1. Introduction

Austenitic stainless steels find widespread application in high-temperature systems owing to their good mechanical properties coupled with adequate endurance in most of the corrosive environments. In fast reactors, the components are in contact with flowing sodium at high temperature. Stainless steel has been reported to possess acceptable compatibility with sodium.[1–6] Hence, a majority of the components of the fast reactors are fabricated using this material. However, some of the constituent elements (being present as interstitial and substitutional alloying elements) dissolve in sodium even though they only exist in trace levels.[7,8] Optimum concentrations of constituent elements are required to sustain good mechanical and corrosion properties, and therefore, the leaching caused by sodium could adversely affect the components.

The corrosive effect of liquid sodium is significantly altered by the presence of certain dissolved impurities. Presence of an impurity such as oxygen in sodium significantly aggravates the corrosion process.[9,10] The generation of ternary compounds such as $NaCrO_2$ promotes the leaching of chromium. This compound is formed even when the oxygen concentration of sodium is very low.[11–14] Ternary compounds of other constituent elements of steel with sodium and oxygen are formed only when the oxygen content is substantially high.[13,14,15] Such very high concentration is normally not encountered in sodium loops, where the concentration of oxygen is controlled through continuous cold trapping.

In order to fully understand the corrosion problems and to suggest optimum operational parameters, several countries of the world have embarked on programs to test materials in sodium environments (*in situ* and off-line). Even though there are a wealth of data generated by different countries, the direct application of these data among different countries is rendered difficult because of the differences in the qualities of sodium used by each country. As already mentioned, corrosion by sodium is strongly dependant on the contents of various dissolved impurities. The present investigation has been designed to unravel the corrosion behavior of AISI type 316LN stainless steel at a temperature of 823 K on exposure to the sodium procured from Indian sources. The duration of exposure was 6,000 h (21.6 Ms).

2. Experimental

2.1 Description of the Loop

The specimens were exposed to flowing sodium in a loop called the "mass-transfer loop." The sodium in the loop was circulated using an electromagnetic pump. The flow rate of sodium was 5 m/s in the test sections. The impurities in sodium were controlled by continuously bypassing a part of sodium through a cold trap. In the cold trap, the impurities are precipitated and retained without being carried to the main loop. The total impurity content in the sodium was determined by a device attached to the purification module. This device was called the "plugging indicator." In this device, sodium was allowed to pass through an orifice. The temperature of the orifice was progressively brought down by cooling it externally by blowing air. The precipitation of impurities results in the reduction of flow of sodium through the orifice. From the data on temperature at

S. Rajendran Pillai, N. Sivai Barasi, H.S. Khatak, and **A.L.E. Terrance,** Materials Characterization Group, Indira Gandhi Centre for Atomic Research; and **R.D. Kale, M. Rajan,** and **K.K. Rajah,** Engineering Development Group, Indira Gandhi Centre for Atomic Research, Kalpakkam, Tamil Nadu, India 603 102.

which the plugging has occurred and dependence of solubility of impurities on temperature, it is possible to gauge the total impurity contents in sodium. The samples to be exposed to sodium were contained in a specially designed sample holder. The sample holder has provisions for simultaneously carrying out thermal aging of the specimen. Comprehensive details about the loop and sample holder have been published in the literature.[1]

2.2 Materials Used

Rectangular plates of stainless steel type AISI 316LN were employed as the specimen. The chemical composition is given in Table 1.

2.3 Mode of Exposure to Sodium

The sample holders with the samples were welded to the appropriate position in the loop. Sodium was allowed to flow along the surface of the sample at a velocity of 5 m/s. The flow of sodium was permitted only through a narrow slit of width 6 mm. The region subjected to the corrosive effect of flowing sodium was cut and specimens for different investigations were prepared.

There were a total of six sample holders in the loop. These were subjected to different temperatures of exposure ranging from 598 to 823 K. The analysis of the specimen from the highest temperature zone in the loop (823 K) was carried out and is discussed in this paper.

2.4 Microstructural Examination

Specimens required for the microstructural investigation were mounted in a mold of adhesive. It was polished using successive grades of silicon carbide-coated paper. It was subsequently polished using diamond paste to a surface finish of 1 μm. The polished surface was etched in a solution of 10% oxalic acid by passing a current of 0.01 A/mm^2 for 120 to 180 s (2 to 3 min). It was subsequently examined under optical and scanning electron microscopes.

2.5 Microhardness

The Vickers hardness numbers (VHN) of the polished specimens were measured under a load of 100 g. The VHN values were obtained at different intervals of depths from the sodium-exposed surface.

2.6 Tensile Behavior

Flat tensile samples were machined from the sodium-exposed specimen. The machining was carried out in such a way that the sodium-exposed region formed the gauge length. Tensile specimens were also fabricated from as-received and thermally aged materials. The tests were carried out using a universal testing machine (Instron Canton, MA) model 1195 at a strain rate of 2.2×10^{-4} s^{-1}.

Table 1 Chemical composition of the material

Element	Cr	Ni	Mo	Mn	Si	C	P	N
Wt.%	16.8	10.4	2.06	1.6	0.53	0.026	0.031	0.073

2.7 Leaching of Elements as Determined by Energy Dispersive Spectroscopy

The concentration of elements on the sodium-exposed surface was determined by energy dispersive x-ray spectrometry (EDS). The specimen was cross-sectionally mounted and the analyses were carried out at fixed depth intervals of 1 μm starting from the edge of the sodium-exposed surface. The intensities of characteristic x-rays emitted by the different elements were estimated with the help of a multichannel analyzer.

2.8 Analysis of phase changes as determined by x-ray diffraction

The phase change brought about by leaching of elements by sodium was determined by x-ray diffraction (XRD). The incident x-rays were Cu K_α.

2.9 Carbon and Nitrogen Profiles

The sodium-exposed specimens was cross-sectionally mounted and analyzed for carbon and nitrogen by electron probe micro analysis (EPMA). By analyzing the intensity of characteristic x-rays emitted by carbon and nitrogen, their concentrations were estimated. The analyses were carried out at periodic depth intervals starting from the edge of the sodium-exposed surface.

3. Results and Discussion

Microstructure of the material in the as-received condition showed a step structure that indicated the fully annealed condition. Thermal aging at 823 K for 6,000 h caused the generation of a sensitized microstructure. As in the case of thermally aged specimens, the specimens exposed to sodium also showed a sensitized microstructure in the matrix. There was continuous carbide precipitate at the grain boundaries. In the region close to the sodium-exposed surface, the precipitation of carbide was more predominant than in the bulk (indicated by a broader grain boundary zone with the precipitate in the region close to the surface). This behavior is attributed to the carburization of steel by the carbon dissolved in sodium. The micrographs of the thermally aged and the surface region of the sodium-exposed specimens are given in Fig. 1.

The sodium-exposed specimen also revealed the generation of a modified region. This layer was similar to the one observed in the case of AISI 316 stainless steel, which was exposed to sodium.[16] The XRD data on the sodium-exposed surface are shown in Fig 2. It revealed the generation of a ferrite phase (the x-ray diffractograms were recorded using a Siemens D-500 powder diffractometer equipped with a diffracted beam monochromator tuned for Cu K_α Siemens, Germany). The fluorescence effects of iron-base alloys have been circumvented in this configuration.

Chemical analysis indicated that the carbon content has increased from 0.026 to 0.032 wt.%. The specimen for chemical analysis was taken from the sodium-exposed zone. The thickness of the specimen was 3 mm and hence the effect of surface carburization was reflected only marginally in this analysis. However, it provided evidence for the carburization undergone by the

material. Measurement of microhardness profile gave further evidence of carburization. The VHN of the sodium-exposed specimen at the surface was substantially higher at 350 when compared to 180 for the thermally aged and as-received materials.

The results obtained by EDS analysis are given in Fig. 3. There was a reduction in the concentration of chromium and nickel in the case of sodium-exposed specimens. The concentration of nickel was very low at the surface (<5 wt. %) and passed through a maximum at a depth of 2 μm from the surface. The concentration was the lowest at a depth of 4 μm and thereafter steadily increased to attain the matrix concentration at a depth of 8 μm. The reason for the variation of concentration of nickel in the above manner could not be fully explained. The depletion of nickel (major element responsible for retaining the austenite structure) caused the generation of ferrite phase at the surface exposed to sodium. Even the increase in the content of carbon (an austenetizing element) could not compensate for the reduction in nickel content and restrict the phase transformation.

The leaching of chromium was significant up to a depth of 2 μm. Thereafter, its concentration steadily increased and attained the matrix value at a depth of 4 μm from the surface. The concentration of iron showed an apparent increase up to a depth of 6 μm because of the reduction in concentration of other elements.

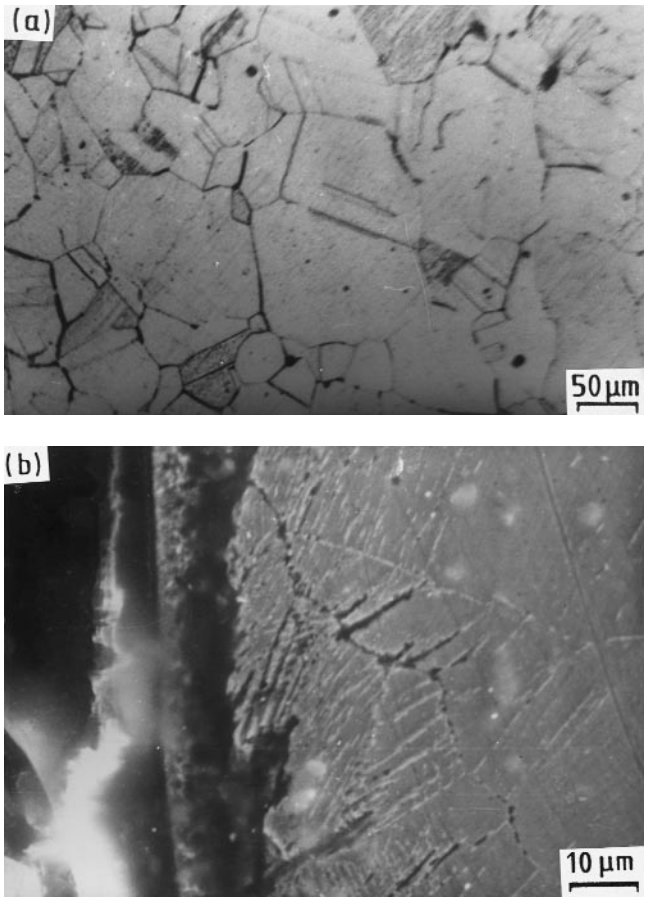

Fig. 1 Microstructures of specimens: **(a)** optical micrograph, thermally aged; and **(b)** micrograph, sodium-exposed scanning electron

The carburization of steel on exposure to sodium was also evident from the EPMA (Fig. 4). The sodium-exposed region formed a carburized layer of thickness 5.5 μm. The maximum content of carbon in the carburized zone was 0.35 wt.% as compared to 0.026 wt.% in the original material. The content of nitrogen in the sodium-exposed surface also showed an increase (Fig. 5; it increased from 0.073 to 0.341 wt.%) at the surface.

The extent of carburization in the present alloy was higher than that reported in the case of AISI type 316 stainless steel

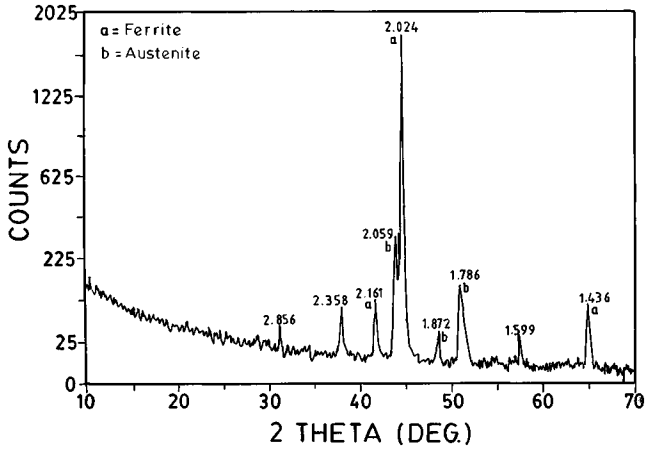

Fig. 2 XRD analysis of the specimen exposed to sodium

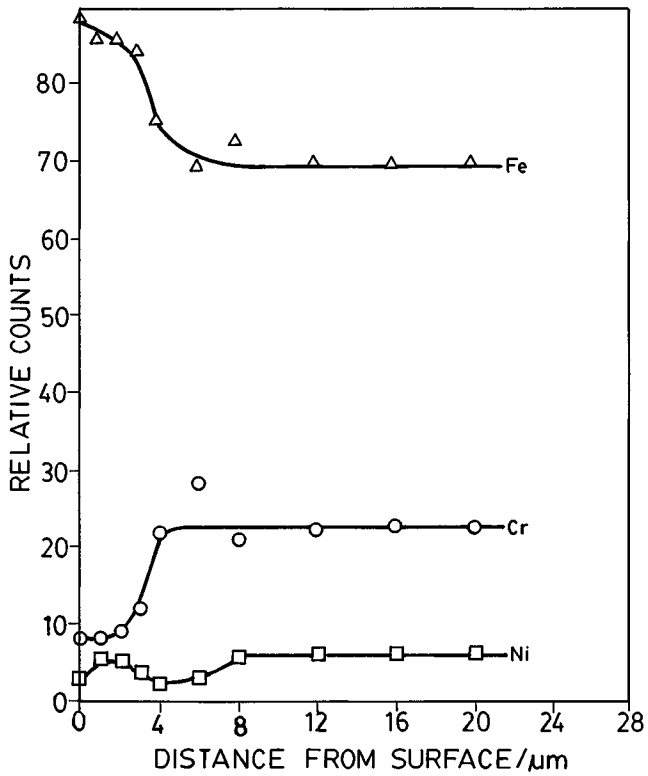

Fig. 3 EDS analysis of leaching of elements from the sodium-exposed surface

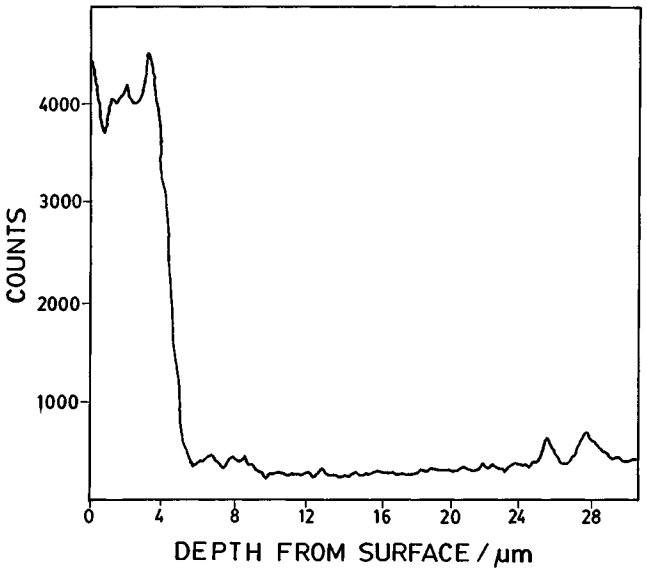

Fig. 4 EPMA concentration profile of carbon on the sodium-exposed region

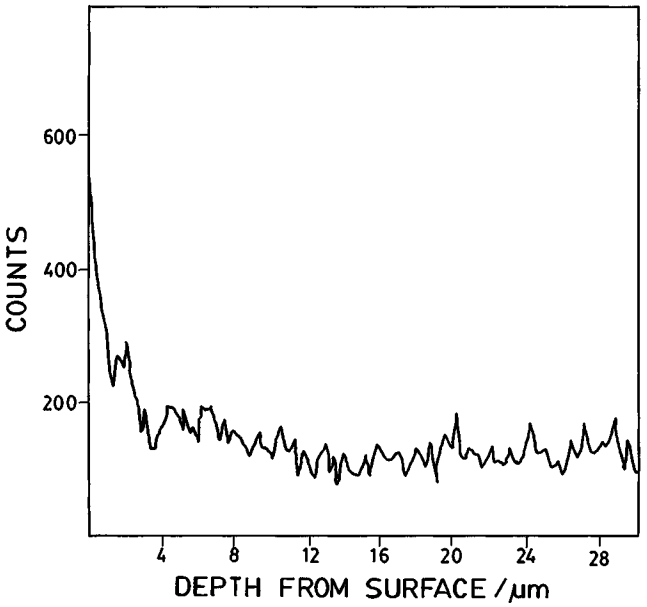

Fig. 5 EPMA concentration profile of nitrogen on the sodium-exposed region

(with carbon content of 0.056 wt.%), which was exposed to some sodium (823 K, 16,000 h).[1] The extensive carburization undergone by this material is presumed to be due to two causes.

- The loop is constructed of AISI 316 stainless steel with a carbon content of 0.06 wt.%. Exposure of AISI 316 LN stainless steel with a carbon content of 0.026 wt.% naturally causes carburization because of a large difference in carbon activity between these alloys. The flowing liquid sodium acted as the transfer medium.
- The generation of cyanide would lead to a high carbon potential in the loop and contribute to higher carburization. It was possible that the nitrogen present in the steel specimens reacted with the carbon dissolved in the sodium to form sodium cyanide. The free energy data of cyanide sheds light on this possibility.[17] The evidence for the existence of cyanide species in sodium has been reported in the literature.[18]

The solubility of sodium cyanide in sodium is very high when compared to other species of carbon encountered in sodium.[19] Hence, this species is very easily transported through sodium from one part of the loop to another. The cyanide species caused the carburization and nitridation of the specimens at the high-temperature zone because of favorable kinetics. Supporting evidence for the carburization and nitridation was obtained by the EPMA. The analysis of the sodium to ascertain the presence of cyanide could not be carried out at present. Its concentration was expected to be below the limit of sensitivity of analytical equipment. However, it was expected to accumulate in the cold trap due to precipitation. Hence, its existence in the sodium system can be confirmed only when cold trap residues are analyzed at a future date.

The tensile data on different specimens are given in Table 2. Thermal aging and exposure to sodium did not cause any appreciable difference in yield strength (YS) and ultimate tensile strength (UTS). However, there was a noticeable reduction in the uniform elongation (UE) and total elongation (TE) at rupture in the case of both thermally aged and sodium-exposed specimens. The reduction in UE was 7% in the case of thermal aging and 19% on exposure to sodium. Corresponding reductions in TE were 10% on thermal aging and nearly 27% on exposure to sodium. This behavior is attributed to the transport of an interstitial element such as carbon and nitrogen across the steel-sodium interface and the subsequent hardening effect. The impact of carburization and nitridation on the YS and UTS were within the experimental scatter and thus could not be clearly established.

Table 2 Tensile data of as-received, thermally aged, and sodium-exposed specimen

Reference	YS (MPa)	UTS (MPa)	UE (%)	TE (%)
As-received	336	606	67	87
	384	625	61	77
Thermally aged	340	655	60	75
	280	645	60	73
Sodium-exposed	389	642	52	62
	363	632	48	58

4. Conclusions

Austenitic stainless steel of the type AISI 316 LN was exposed to flowing sodium in a loop at a temperature of 823 K for 6,000 h. These specimens were retrieved from the loop and analyzed for the different changes brought about by mass transfer through sodium. The main conclusions drawn from this investigation are as follows.

- Thermal aging at 823 K caused the generation of carbide precipitate at the grain boundaries. The specimen exposed to sodium revealed increased precipitation of carbon because of carburization by the carbon dissolved in sodium.
- Exposure to sodium caused the leaching of elements such as chromium and nickel.
- The surface hardness of the sodium-exposed specimen was enhanced because of carburization and nitridation.
- Exposure to sodium caused the generation of a modified layer, which contained ferrite. This transformation was driven by the loss of the austenite stabilizing element, nickel.

Acknowledgments

The authors wish to acknowledge with thanks Dr. S.V. Sasthry, Materials Science Div., for the XRD analysis; and Mrs. Radhika and Mr. Thomas Paul, Materials Characterization Group, for their help in various instrumental analyses.

References

1. S. Rajendran Pillai, H.S. Khatak, N. Sivai Barasi, A.K. Tyagi, J.B. Gnanamoorthy, R.D. Kale, K. Swaminathan, M. Rajan and K.K. Rajan: Trans. Ind. Inst. Met., 1997, vol. 50, p. 103-10.
2. K. Natesan, T.F. Kassnen, and Che-Yu-Li: *Reactor Technol.*, 1972, vol. 15 (4), pp. 244-77.
3. S. Rajendran Pillai, H.S. Khatak, and J.B. Gnanamoorthy: *Mater. Trans. JIM*, 1998, vol. 39 (3), pp. 370-77.
4. Y. Wada, T. Asayama, and R. Komine: *Int. Atomic Energy Specialist Meeting*, KFK-4935, IWGFR/84, Forschungszentrum Karlsruhe, IAEA, 1991, pp. 149-59.
5. H.U. Borgstedt and H. Huthmann: *J. Nucl. Mater.*, 1991, vol. 183, pp. 127-36.
6. J.L. Krankota: *J. Eng. Mater. Technol.* 1976, Jan, p. 9-16.
7. T.D. Claar: *Reactor Technol.*, 1970, vol. 13, pp. 124-46.
8. B. Longson and A.W. Thorley: *J. Appl. Chem.*, 1970, vol. 20, pp. 372-79.
9. B.H. Kolster, J.V.D. Veer, and L. Bos: in *Materials Behaviour and Physical Chemistry in Liquid Metal Systems*, H.U. Borgstedt, ed., Plenum Press, New York, NY, 1981, pp. 37-48.
10. M.G. Barker and D.J. Wood: *J. Less-Common Met.*, 1974, vol. 35, pp. 315-23.
11. A.W. Thorley, A. Bhundell, and J.A. Bradsley: in *Materials Behaviour and Physical Chemistry in Liquid Metal Systems*, H.U. Borgstedt, ed., Plenum Press, New York, NY, 1982, pp. 5-18.
12. S. Rajendran Pillai, H.S. Khatak, and J.B. Gnanamoorthy: *J. Nucl. Mater.*, 1995, vol. 224, pp. 17-24.
13. A.M. Azad, O.M. Sreedharan, and J.B. Gnanamoorthy: *J. Nucl. Mater.*, 1987, vol. 144, pp. 94-104.
14. A.M. Azad, O.M. Sreedharan, and J.B. Gnanamoorthy: *J. Nucl. Mater.*, 1998, vol. 151, pp. 292-300.
15. A.W. Thorley and C. Tyzack: *Proc. Liquid Alkali Metals*, BNES, London, 1973, paper no. 41.
16. S. Rajendran Pillai, H.S. Khatak, J.B. Gnanamoorthy, S. Velmurugan, A.K. Tyagi, R.D. Kale, K. Swaminathan, M. Rajan and K.K. Rajan: *Mater. Sci. Technol.*, 1997, vol. 13, pp. 937-43.
17. *J.A.N.A.F. Thermochemical Tables*, National Bureau of Standards, Gaithersburg, MD, 1971.
18. S. A. Shiels and C.Bagnall: in *Materials Behaviour and Physical Chemistry in Liquid Metal Systems*, H.U. Borgstedt, ed., Plenum Press, New York, NY, 1982, pp. 493-502.
19. E. Veleckis, K.E. Anderson, F.A. Cafasso, and H.M. Feder: "Solubilities of Nitrogen Gas and Sodium Cyanide in Liquid Sodium," Report No. ANL-7520, Argonne National Laboratory, Argonne, IL, 1968, pp. 295-98.